Description

[LC COIL]

BACKGROUND

[0001] In magnetic resonance imaging, the rate of data acquisition is limited by how rapidly fields can be changed within the field of view. However, bounds are generally placed on how rapidly fields can be changed within an often larger region, such as a patient. With reduced fields outside the field of view, data acquisition can be acclerated.

SUMMARY

[0002] This invention provides a coil for a magnetic resonance imaging machine with two adjacent regions carrying different currents at the interface. Currents in the two regions at the interface can be in opposite directions.

[0003] The interface separating the two adjacent regions can be planar and the regions can be mirror images of each other across the interface. Current in one region and the opposite of current in the other region can be mirror images of each other across the planar interface. The current den-

sity, or volume current density integrated over the thickness of the coil, can be constant in each region.

[0004] The two adjacent regions of the coil can pass directly under and conform to a support surface, which can be flat. The cross-section of the coil can contain an arc of a circle.

BRIEF DESCRIPTION OF THE FIGURES

[0005] FIG. *1* shows the first embodiment of the coil, side view (FIG. *1*A) and axial view (FIG. *1*B).

[0006] FIG. *2* shows the second embodiment of the coil, side view (FIG. *2*A) and axial view (FIG. *2*B).

DETAILED DESCRIPTION

[0007] FIG. *1* shows a coil within a magnetic resonance imaging machine *10*. The coil has region *3* carrying current *5* and adjacent region *4* carrying current *6*. Currents *5* and *6* differ at the interface *7* between the regions *3* and *4*. The coil has a flat lower part *8* passing under a support surface *9* of the magnetic resonance imaging machine *10* and a partial cylindrical upper part *11* with axis *12*.

[0008] Throughout this specification, the term "LC coil" refers to this invention, the terms "axial", "

▨

direction", and "along

Z

" refer to the direction of a specified axis of the LC coil, and "LC_z coil" refers to an LC coil designed to produce an axial gradient of an axial magnetic field. Terms "LC_x coil" and "LC_y coil" refer to LC coils designed to produce gradients of an axial magnetic field orthogonal to the axis. The term "scanner" refers to a magnetic resonance imaging machine.

1 First Embodiment

[0009]   The first embodiment (FIG. *1*) of an LC_z coil has region *3* carrying current *5* and adjacent region *4* carrying current *6*. Currents *5* and *6* differ at the interface *7* between the regions *3* and *4*. The first embodiment has a flat lower part

S_1

8 passing a distance

Δy

under a flat support surface *9* of a scanner *10* and upper part

S_2

11 a partial cylinder of radius

R

, angle

$$(1 + 2\varepsilon_\varphi)\pi$$

,

$$\varepsilon_\varphi \in [0, 1/2]$$

, and axis *12* coinciding with the scanner axis *13*. The axis *12* is also called the coil axis. The length of the first embodiment along its axis *12* is

$$l_z$$

and the dimension of

$$S_1$$

8 are

$$l_x \times l_z$$

, with

$$l_x < 2R$$

. The distance between

$$S_1$$

8 and the axis *12* is

$$y_c$$

. A surface detection coil 14 is located between

$$S_1$$

8 and the support surface 9.

1.1 DEFINITION OF COORDINATES

[0010] Define rectangular coordinates

$$(x, y, z)$$

with

$$x$$

parallel the support surface 9,

$$y$$

perpendicular to the support surface 9, and

$$z$$

along the coil axis 12. The flat section

$$S_1$$

8 is in the plane

$$y = -y_c$$

and is parallel to the support surface 9 in the plane

$$y = -y_c + \Delta_y$$

. The plane

$$x = 0$$

perpendicular to the support surface *9* contains the coil axis *12* given by the line

$$x = 0$$

and

$$y = 0$$

. Centers of fields of view are arranged to lie within the plane

$$z = 0$$

.

[0011] Cylindrical coordinates

$$(r, \varphi, z)$$

are related to coordinates

$$(x, y, z)$$

by the transformation

$$x = r\cos\varphi \qquad (1a)$$
$$y = r\sin\varphi \qquad (1b)$$

The inverse transformation is

$$r = \sqrt{x^2 + y^2} \qquad (2a)$$
$$\varphi = \cos^{-1}\frac{x}{r} = \sin^{-1}\frac{y}{r} \qquad (2b)$$

The partial cylindrical section

$$S_2$$

11 is at

$$r = R$$

and covers the angular range

$$\varphi \in I_\varphi = \left[-\varepsilon_\varphi \pi \,,\, (1 + \varepsilon_\varphi)\,\pi \right] \tag{3}$$

[0012] The coil dimensions

$$l_x = 2R\cos\left(\varepsilon_\varphi \pi\right) \tag{4a}$$

and

$$y_c = R\sin\left(\varepsilon_\varphi \pi\right) \tag{4b}$$

[0013]

1.2 CURRENT DENSITY

[0014] The coil carries a current density

$$\vec{J}\left(\vec{r}\right) = \begin{cases} J(z)\,\hat{x} & , & \vec{r} \in S_1 \\ J(z)\,\hat{\varphi} & , & \vec{r} \in S_2 \end{cases} \tag{5}$$

where

$$J(z)$$

is the current density profile and

$$\vec{r} = (x, y, z) \tag{6}$$

1.3 FIELD

[0015] Using the Biot–Savart law, the total field

$$B(x, y, z) = \int_{-l_z/2}^{l_z/2} dz' \, J(z') \, g(x, y, z - z') \qquad (7)$$

with

$$
\begin{aligned}
g(x, y, z) &= \frac{\mu_0 (y + y_c)}{4\pi} \int_{-l_x/2}^{l_x/2} dx' \\
&\qquad \frac{1}{\left[(x - x')^2 + (y + y_c)^2 + z^2\right]^{3/2}} \\
&\quad + \frac{\mu_0 R}{4\pi} \int_{I_\varphi} d\varphi' \\
&\qquad \frac{R - r \cos(\varphi - \varphi')}{\left[R^2 + r^2 - 2Rr \cos(\varphi - \varphi') + z^2\right]^{3/2}}
\end{aligned}
$$
$$(8)$$

Under conditions

$$|x|, |y + y_c| \ll l_x/2 \qquad (9a)$$
$$|y + y_c| \ll l_z/2 \qquad (9b)$$
$$\sqrt{x^2 + y^2} \ll R \qquad (9c)$$

the function

$$
\begin{aligned}
g(x, y, z) &\approx \frac{\mu_0}{2\pi} \frac{y + y_c}{(y + y_c)^2 + z^2} \\
&\quad + \frac{\mu_0}{4\pi} \frac{R^2}{[R^2 + z^2]^{3/2}} \left[(1 + 2\varepsilon_\varphi) \pi \right. \\
&\qquad \left. + \frac{l_x \, y \sqrt{x^2 + y^2}}{R^3} \left(\frac{3R^2}{R^2 + z^2} - 1 \right) \right]
\end{aligned}
\qquad (10)
$$

[0016]   If the projection of the field of view onto the

$x - y$

plane is a rectangle

$$L_x \times L_y$$

centered about

$$(x_0, y_0)$$

under conditions

$$L_x/2, |x_0| \ll R \tag{11a}$$

$$L_y/2, |y_0| \ll R, l_z/2 \tag{11b}$$

and

$$y_0 > -y_c + \Delta_y + L_y/2 \tag{11c}$$

and the coil parameter

$$y_c \ll R, l_z/2 \tag{12}$$

then conditions (9) are satisfied within the field of view.

1.4 FIELD WITH (14)

[0017] Define the function sgn by

$$\operatorname{sgn} z = \begin{cases} 1, & z \geq 0 \\ -1, & z < 0 \end{cases} \tag{13}$$

Under conditions (9) with

$$J(z) = J_0 \operatorname{sgn} z \tag{14}$$

the field

$$B(x, y, z) \approx b(x, y, z)$$
$$-\frac{1}{2}\left[b(x, y, z - l_z/2) + b(x, y, z + l_z/2)\right] \tag{15a}$$

with

$$b(x, y, z) = \frac{\mu_0 J_0}{\pi} \text{Tan}^{-1} \frac{z}{y + y_c}$$
$$+ \frac{\mu_0 J_0 z}{2\sqrt{R^2 + z^2}} \left[(1 + 2\varepsilon_\varphi) \right.$$
$$\left. + \frac{l_x y \sqrt{x^2 + y^2}}{\pi R} \left(\frac{1}{R^2} + \frac{1}{R^2 + z^2} \right) \right]$$

$$(15b)$$

using (2a).

[0018] Under conditions (9) and

$$|z| \ll l_z / 2, R \qquad (16)$$

with (14), the field

$$B(x, y, z) \approx \frac{\mu_0 J_0}{\pi} \text{Tan}^{-1} \frac{z}{y + y_c} \qquad (17)$$

the gradient

$$G_z = \left. \frac{\partial B}{\partial z} \right|_{(x,y,z)=(x_0,y_0,0)} \qquad (18a)$$
$$\approx \frac{\mu_0 J_0}{\pi (y_0 + y_c)} \qquad (18b)$$

2 SECOND EMBODIMENT

[0019] The second embodiment (FIG. 2) of an LC_z coil has region 15 carrying current 17 and adjacent region 16 carrying current 18. Currents 17 and 18 differ at the interface 19 between the regions 15 and 16. The second embodiment has a flat upper part

S_1

20 passing a distance

Δ_y

under a flat support surface *21* of a scanner *22* and lower
part

S_2

23 a partial cylinder of radius

R

, angle

$$\left(1 + 2\varepsilon_\varphi\right)\pi$$

,

$$\varepsilon_\varphi \in [0, 1/2]$$

, and axis *24* coinciding with the scanner axis *25*. The axis
25 is also called the coil axis. The length of the second
embodiment along its axis *24* is

l_z

and the dimension of

S_1

20 are

$$l_x \times l_z$$

, with

$$l_x < 2R$$

. The distance between

$$S_1$$

20 and the axis *24* is

$$y_c$$

. A surface detection coil *26* is located between

$$S_1$$

20 and the support surface *21*

2.1 DEFINITION OF COORDINATES

[0020]   Define rectangular coordinates

$$\left(x, y, z \right)$$

with

$$x$$

parallel the support surface *21*,

$$y$$

perpendicular to the support surface *21*, and

$$z$$

along the coil axis *24*. The flat section

S_1

20 is in the plane

$$y = -y_c$$

and is parallel to the support surface *21* in the plane

$$y = -y_c + \Delta_y$$

. The plane

$$x = 0$$

perpendicular to the support surface *21* contains the coil

axis *24* given by the line

$$x = 0$$

and

$$y = 0$$

. Centers of fields of view are arranged to lie within the

plane

$$z = 0$$

.

[0021] Cylindrical coordinates

$$(r, \varphi, z)$$

are related to coordinates

$$(x, y, z)$$

by the transformation (1). The inverse transformation is (2). The partial cylindrical section

$$S_2$$

23 is at

$$r = R$$

and covers the angular range

$$\varphi \in I_\varphi = \left[-\left(1 - \varepsilon_\varphi\right)\pi, \ -\varepsilon_\varphi \pi\right] \qquad (19)$$

[0022] The coil dimensions

$$l_x$$

and

$$y_c$$

are given by (4a) and (4b).

2.2 CURRENT DENSITY

[0023] The coil carries a current density

$$\vec{J}\left(\vec{r}\right) = \begin{cases} J\left(z\right)\hat{x} & , & \vec{r} \in S_1 \\ -J\left(z\right)\hat{\varphi} & , & \vec{r} \in S_2 \end{cases} \qquad (20)$$

where

$$J\left(z\right)$$

is the current density profile.

2.3 Field

[0024]   The first and second embodiments have different partial cylindrical sections S_2' 11 and S_2' 23: current densities (5) and (20) for

$$\vec{r} \in S_2'$$

are carried in complementary angular ranges (3) and (19). Expressions for the field produced by the second embodiment can be obtained by modifying the expressions of Sec. (1.3).

[0025]   The field

$$B(x,y,z) = \int_{-l_z/2}^{l_z/2} dz' J(z') g(x, y, z - z') \qquad (21)$$

with

$$g(x,y,z) = \frac{\mu_0(y+y_c)}{4\pi}\int_{-l_x/2}^{l_x/2}dx'$$

$$\frac{1}{\left[(x-x')'^2+(y+y_c)^2+z^2\right]^{3/2}}$$

$$-\frac{\mu_0 R}{4\pi}\int_{I_\varphi}d\varphi'$$

$$\frac{R-r\cos(\varphi-\varphi')}{\left[R^2+r^2-2Rr\cos(\varphi-\varphi')+z^2\right]^{3/2}} \quad (22)$$

n

can be expressed in terms of

x

and

y

using (2a). Under conditions (9),

$$g(x,y,z) \approx \frac{\mu_0}{2\pi}\frac{y+y_c}{(y+y_c)^2+z^2}$$

$$-\frac{\mu_0}{4\pi}\frac{R^2}{[R^2+z^2]^{3/2}}\left[(1-2\varepsilon_\varphi)\pi\right.$$

$$\left.+\frac{l_x\,y\sqrt{x^2+y^2}}{R^3}\left(\frac{3R^2}{R^2+z^2}-1\right)\right] \quad (23)$$

[0026] If the projection of the field of view onto the

$x-y$

plane is a rectangle

$$L_x \times L_y$$

centered about

$$(x_0, y_0)$$

under conditions (11) and the coil parameter

$$y_c$$

satisfies (12), then conditions (9) are satisfied within the field of view.

2.4 FIELD WITH (14)

[0027] Expressions for the field and gradient produced by the second embodiment can be obtained by modifying the expressions of Sec. (1.4).

[0028] Under conditions (9) with (14), the field

$$B(x, y, z) \approx b(x, y, z)$$
$$- \frac{1}{2} \left[b(x, y, z - l_z/2) + b(x, y, z + l_z/2) \right] \tag{24a}$$

with

$$b\left(x,y,z\right) = \frac{\mu_0 J_0}{\pi} \text{Tan}^{-1} \frac{z}{y+y_c}$$
$$-\frac{\mu_0 J_0 z}{2\sqrt{R^2+z^2}} \left[(1-2\varepsilon_\varphi) \right.$$
$$\left. +\frac{l_x y \sqrt{x^2+y^2}}{\pi R} \left(\frac{1}{R^2} + \frac{1}{R^2+z^2}\right) \right]$$

(24b)

[0029] Under conditions (9) and (16) with (14), the field

B

is (17) and the gradient

G_z

is (18)

3 MRI USING AN LC COIL

[0030]

3.1 FIELD PROFILES

[0031] The three types of LC coil are LC_x, LC_y, and LC_z. An LC_x coil produces an LC_x field

$$B\left(\vec{r}, t\right) = G_x\left(t\right) \tilde{x}\left(\vec{r}\right)$$

(25a)

with gradient

$$G_x = \frac{\partial B}{\partial x}$$

(25b)

An LC_y coil produces an LC_y field

$$B\left(\vec{r}, t\right) = G_y\left(t\right) \tilde{y}\left(\vec{r}\right)$$

(26a)

with gradient

$$G_y = \frac{\partial B}{\partial y} \tag{26b}$$

An LC$_z$ coil produces an LC$_z$ field
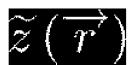
$$B\left(\overrightarrow{r}, t\right) = G_z\left(t\right) \tilde{z}\left(\overrightarrow{r}\right) \tag{27a}$$

with gradient

$$G_z = \frac{\partial B}{\partial z} \tag{27b}$$

The gradients are evaluated at the center of the field of view.

[0032] Magenetic resonance imaging with an LC$_z$ coil requires that

$$\tilde{z}\left(\overrightarrow{r}\right)$$

satisfy

$$
\begin{aligned}
\tilde{z} &= 0 \text{ at the center of the field of view} &\text{(28a)}\\
\partial \tilde{z}/\partial z &= 1 \text{ at the center of the field of view} &\text{(28b)}\\
\partial \tilde{z}/\partial z &> 0 \text{ within the field of view} &\text{(28c)}
\end{aligned}
$$

and

$$
\begin{aligned}
&\tilde{z} \text{ attains values for fixed } x \text{ and } y \text{ within the}\\
&\text{field of view that are unique within the region}\\
&\text{of sensitivity of the detection coil} \qquad\qquad \text{(28d)}
\end{aligned}
$$

Magnetic resonance imaging with an LC$_x$ coil requires that

$$\tilde{x}\left(\overrightarrow{r}\right)$$

satisfy (28) with

$$x \longleftrightarrow z$$

and

$$\tilde{x} \longleftrightarrow \tilde{z}$$

. Magnetic resonance imaging with an LC$_y$ coil requires that

$$\tilde{y}\left(\vec{r}\right)$$

satisfy (28) with

$$y \longleftrightarrow z$$

and

$$\tilde{y} \longleftrightarrow \tilde{z}$$

.

[0033] The center of a field of view refers to the center of an image in field coordinates. For example, if fields linear in

$$\tilde{x}$$

and

$$\tilde{y}$$

are used with an LC$_z$ field linear in

$$\tilde{z}$$

, the field of view is a rectangular box in field coordinates

$$\left(\tilde{x}, \tilde{y}, \tilde{z}\right)$$

and the center of the field of view refers to the center of the box.

3.2 IMAGING PARAMETERS

[0034] This section assumes the use of an LC_z field together with fields linear in

$$\tilde{x}$$

and

$$\tilde{y}$$

. Similar equations hold for other combinations of LC and linear fields.

3.2.1 NON-OBLIQUE IMAGING PARAMETERS

[0035] In field coordinates

$$(x, y, \tilde{z})$$

, the field of view is a box

$$L_x \times L_y \times \tilde{L}_z$$

centered about

$$(x, y, \tilde{z}) = (x_0, y_0, 0) \Leftrightarrow (x, y, z) = (x_0, y_0, z_0) \qquad (29)$$

With choices for pixel numbers

$$N_x, N_y, N_z$$

, and pixel sizes

$$\Delta x, \Delta y, \Delta z$$

, the imaging parameters are

$$L_x = N_x \Delta x \tag{30a}$$
$$L_y = N_y \Delta y \tag{30b}$$
$$\widetilde{L}_z = N_z \Delta z \tag{30c}$$

$$k_x = n_x \Delta k_x \tag{31a}$$
$$k_y = n_y \Delta k_y \tag{31b}$$
$$k_z = n_z \Delta k_z \tag{31c}$$

$$n_x \in \{-N_x/2, \ldots, N_x/2 - 1\} \tag{32a}$$
$$n_y \in \{-N_y/2, \ldots, N_y/2 - 1\} \tag{32b}$$
$$n_z \in \{-N_z/2, \ldots, N_z/2 - 1\} \tag{32c}$$

$$\Delta k_x = \frac{2\pi}{L_x} \tag{33a}$$
$$\Delta k_y = \frac{2\pi}{L_y} \tag{33b}$$
$$\Delta k_z = \frac{2\pi}{\widetilde{L}_z} \tag{33c}$$

[0036] Fourier reconstruction yields an image on a grid in field coordinates:

$$(x, y, \tilde{z}) = (n_x \Delta x + x_0, \ n_y \Delta y + y_0, \ n_z \Delta z) \tag{34}$$

The image can be scaled to coordinates

$$\left(x, y, z \right)$$

using the 1-to-1 mapping

$$(x, y, z) \leftrightarrow (x, y, \tilde{z}) \quad \text{within } F \cap D \tag{35}$$

The resolutions in coordinates

$$(x, y, z)$$

are accurately given by

$$(\Delta x, \Delta y, \Delta z)\, \mathbf{J}' = \left(\Delta x, \Delta y, \Delta z\, (\partial \tilde{z}/\partial z)^{-1}\right) \qquad (36)$$

where Jacobian

$$\mathbf{J}' = \frac{\partial (x, y, z)}{\partial (x, y, \tilde{z})} = \begin{bmatrix} 1 & 0 & 0 \\ 0 & 1 & 0 \\ 0 & 0 & (\partial \tilde{z}/\partial z)^{-1} \end{bmatrix} \qquad (37)$$

using the relation

$$\partial z/\partial \tilde{z} = (\partial \tilde{z}/\partial z)^{-1} \qquad (38)$$

which follows from the fact that both

$$\partial z/\partial \tilde{z}$$

and

$$\partial \tilde{z}/\partial z$$

are taken at constant

$$x$$

and

$$y$$

. At the center of the field of view (29), the Jacobian

$$\mathbf{J}'$$

is the identity matrix and the resolutions are

$$\Delta x, \Delta y, \Delta z$$

.

3.2.2 DOUBLE-OBLIQUE IMAGING PARAMETERS

[0037] Coordinates

$$\left(x', y', z' \right)$$

and field coordinates

$$\left(\tilde{x}', \tilde{y}', \tilde{z}' \right)$$

are obtained from coordinates

$$\left(x, y, z \right)$$

and field coordinates

$$\left(x, y, \tilde{z} \right)$$

by a rotation by

$$\theta_1$$

about

$$z$$

and a rotation by

$$\theta_2$$

about

x

:

$$(x', y', z') = (x, y, z)\, R \Leftrightarrow (x, y, z) = (x', y', z')\, R^{-1} \tag{39}$$

and

$$(\tilde{x}', \tilde{y}', \tilde{z}') = (x, y, \tilde{z})\, R \Leftrightarrow (x, y, \tilde{z}) = (\tilde{x}', \tilde{y}', \tilde{z}')\, R^{-1} \tag{40}$$

where the rotation matrix

$$R = \begin{bmatrix} \cos\theta_1 & -\sin\theta_1 & 0 \\ \sin\theta_1 \cos\theta_2 & \cos\theta_1 \cos\theta_2 & -\sin\theta_2 \\ \sin\theta_1 \sin\theta_2 & \cos\theta_1 \sin\theta_2 & \cos\theta_2 \end{bmatrix} \tag{41}$$

and inverse matrix

$$R^{-1} = \begin{bmatrix} \cos\theta_1 & \sin\theta_1 \cos\theta_2 & \sin\theta_1 \sin\theta_2 \\ -\sin\theta_1 & \cos\theta_1 \cos\theta_2 & \cos\theta_1 \sin\theta_2 \\ 0 & -\sin\theta_2 & \cos\theta_2 \end{bmatrix} \tag{42}$$

[0038] Consider combining fields linear in

x

,

y

, and

z

according to (40) to create fields linear in

$\tilde{x}'$

,

$$\widetilde{y}'$$

, and

$$\widetilde{z}'$$

. In field coordinates

$$\left(\widetilde{x}', \widetilde{y}', \widetilde{z}'\right)$$

, the field of view is a box

$$\widetilde{L}_{x'} \times \widetilde{L}_{y'} \times \widetilde{L}_{z'}$$

centered about

$$
\begin{aligned}
(x, y, \widetilde{z}) = (x_0, y_0, 0) &\Leftrightarrow (\widetilde{x}', \widetilde{y}', \widetilde{z}') = (\widetilde{x}_0', \widetilde{y}_0', \widetilde{z}_0') \\
&\Leftrightarrow (x', y', z') = (x_0', y_0', z_0')
\end{aligned}
\tag{43}
$$

With choices for pixel numbers

$$N_{x'}, N_{y'}, N_{z'}$$

, and pixel numbers

$$\Delta x', \Delta y', \Delta z'$$

, the imaging parameters are

$$
\begin{aligned}
\widetilde{L}_{x'} &= N_{x'} \Delta x' & \text{(44a)} \\
\widetilde{L}_{y'} &= N_{y'} \Delta y' & \text{(44b)} \\
\widetilde{L}_{z'} &= N_{z'} \Delta z' & \text{(44c)}
\end{aligned}
$$

$$k_{x'} = n_{x'} \Delta k_{x'} \qquad (45a)$$

$$k_{y'} = n_{y'} \Delta k_{y'} \qquad (45b)$$

$$k_{z'} = n_{z'} \Delta k_{z'} \qquad (45c)$$

$$n_{x'} \in \{-N_{x'}/2, \ldots, N_{x'}/2 - 1\} \qquad (46a)$$

$$n_{y'} \in \{-N_{y'}/2, \ldots, N_{y'}/2 - 1\} \qquad (46b)$$

$$n_{z'} \in \{-N_{z'}/2, \ldots, N_{z'}/2 - 1\} \qquad (46c)$$

$$\Delta k_{x'} = \frac{2\pi}{\tilde{L}_{x'}} \qquad (47a)$$

$$\Delta k_{y'} = \frac{2\pi}{\tilde{L}_{y'}} \qquad (47b)$$

$$\Delta k_{z'} = \frac{2\pi}{\tilde{L}_{z'}} \qquad (47c)$$

[0039] Fourier reconstruction yields an image on a grid:

$$(\tilde{x}', \tilde{y}', \tilde{z}') = (n_{x'} \Delta x' + \tilde{x}'_0, \; n_{y'} \Delta y' + \tilde{y}'_0, \; n_{z'} \Delta z' + \tilde{z}'_0) \qquad (48)$$

The image can be scaled to coordinates

$$(x', y', z')$$

using the 1-1 mapping (35) and the transformations (39) and (40):

$$(\tilde{x}', \tilde{y}', \tilde{z}') \rightarrow (x, y, \tilde{z}) \rightarrow (x, y, z) \rightarrow (x', y', z') \qquad (49)$$

The resolutions in coordinates

$$(x', y', z')$$

are accurately given by

$$(\Delta x', \Delta y', \Delta z') \tilde{\mathbf{J}}' \qquad (50)$$

where Jacobian

$$\tilde{\mathbf{J}}' = R^{-1}\mathbf{J}'R \qquad (51)$$

At the center of the field of view (43), the Jacobians

$$\mathbf{J}'$$

and

$$\tilde{\mathbf{J}}'$$

are the identity matrices and the resolutions

$$\Delta x', \Delta y', \Delta z'$$

.

3.3 ADDITIONAL PARAMETERS

[0040] The parameter

$$\kappa$$

is defined by

$$\kappa = \frac{|B|_{\max_P}}{|B|_{\max_{F \cap D \cap P}}} > 1 \qquad (52)$$

where

$$B\big|_{\max_P}$$

and

$$B\big|_{\max_{F \cap D \cap P}}$$

indicate the maximum values of

$$B$$

attained over a region

$$P$$

, such as a patient, and over the intersection

$$F \cap D \cap P$$

, where

$$F$$

is the field of view and

$$D$$

is the region of sensitivity of the detection coil. A second parameter

$$\kappa_D$$

is defined by

$$\kappa_D = \frac{|B|_{\max_{D \cap P}}}{|B|_{\max_{F \cap D \cap P}}} \in [1, \kappa] \qquad (53)$$

4 MRI USING FIRST AND SECOND EMBODIMENTS

[0041]

4.1 FIELD COORDINATE WITH (14)

[0042] The current densities of the first and second embodiments are (5) and (20). Under conditions (9) and (16) with

(14), the field is (17) and field coordinate

$$\tilde{z} = \frac{B}{G_z} \quad (54a)$$

$$\approx (y_0 + y_c) \operatorname{Tan}^{-1} \frac{z}{y + y_c} \quad (54b)$$

Within a field of view

$$F$$

that is a rectangular box

$$L_x \times L_y \times \tilde{L}_z$$

in coordinates

$$(x, y, \tilde{z})$$

centered about

$$(x_0, y_0, 0)$$

, (9) is satisfied given (11) and (12), and (16) is satisfied given

$$|z|_{\max F} = \left(\frac{L_y}{2} + y_0 + y_c \right) \tan \frac{L_z}{2 (y_0 + y_c)} \ll l_z/2, R \quad (55a)$$

and

$$\tilde{L}_z < \pi (y_0 + y_c) \quad (55b)$$

The field coordinate

$$\tilde{z}$$

(54) then satisfies (28).

4.2 IMPROVED FIELDS

[0043] The ideal LC$_z$ field

$$B^{\text{id}}\left(\vec{r}, t\right) = G_z \tilde{z}^{\text{id}}\left(z; \tilde{L}_z\right) \tag{56}$$

where the field coordinate

$$\tilde{z}^{\text{id}}\left(z; \tilde{L}_z\right) = \begin{cases} \tilde{L}_z/2 & , & z > \tilde{L}_z/2 \\ z & , & z \in \left[-\tilde{L}_z/2, \tilde{L}_z/2\right] \\ -\tilde{L}_z/2 & , & z < -\tilde{L}_z/2 \end{cases} \tag{57}$$

For a field of view with

$$\tilde{z}^{\text{id}} \in \left[-\tilde{L}_z/2, \tilde{L}_z/2\right]$$

, the field

$$B^{\text{id}}$$

has the values

$$\kappa = \kappa_D = 1$$

and a uniform resolution

$$\Delta z \left(\partial \tilde{z}/\partial z\right)^{-1}$$

(36) along

$$\hat{z}$$

for

$$z \in \left[-\tilde{L}_z/2, \tilde{L}_z/2 \right]$$

.

[0044] Curent density profiles

$$J\left(z\right)$$

that produce fields

$$B$$

better approximating the ideal fields

$$B^{\text{id}}$$

(56) over

$$D$$

than (17) can be calculated. The field

$$B\left(x_0, y_0, z\right)$$

is given by (7), where

$$g\left(x_0, y_0, z\right)$$

is (8) for the first embodiment and (22) for the second embodiment. The integral (7) can be approximated by a sum:

$$B_i \approx \delta z \sum_{j=-n}^{n} g_{i-j} J_j \qquad (58)$$

where

$$
\begin{aligned}
B_j &= B(x_0, y_0, j\delta z) & \text{(59a)} \\
J_j &= J(j\delta z) & \text{(59b)} \\
g_j &= g(x_0, y_0, j\delta z) & \text{(59c)}
\end{aligned}
$$

and

$$J(z)$$

either vanishes or is neglected for

$$|z| > n\delta z$$

.

[0045] Defining the matrix

$$\mathbf{G}_{ij} = \delta z \, g_{i-j} \qquad \text{(60)}$$

and treating

$$B_j$$

and

$$J_j$$

as column vectors, the approximation (58) becomes the matrix equation

$$B_i \approx \sum_{j=-n}^{n} \mathbf{G}_{ij} J_j \qquad \text{(61)}$$

[0046] For the first embodiment

$$\mathbf{G}_{ij} \underset{(8)}{=} \frac{\mu_0 Y \delta z}{4\pi} \int_{-l_x/2}^{l_x/2} dx'$$

$$\frac{1}{\left[X^2 + Y^2 + (\delta z)^2 (i-j)^2\right]^{3/2}}$$

$$+ \frac{\mu_0 R \delta z}{4\pi} \int_{I_\varphi} d\varphi'$$

$$\frac{R - r_0 \cos \Phi}{\left[R^2 + r_0^2 - 2Rr_0 \cos \Phi + (\delta z)^2 (i-j)^2\right]^{3/2}} \tag{62}$$

where

$$X = x_0 - x' \tag{63a}$$

$$Y = y_0 + y_c \tag{63b}$$

$$\Phi = \varphi_0 - \varphi' \tag{63c}$$

$$r_0 = \sqrt{x_0^2 + y_0^2} \tag{63d}$$

$$\varphi_0 = \cos^{-1} \frac{x_0}{r_0} = \sin^{-1} \frac{y_0}{r_0} \tag{63e}$$

Both terms are decreasing functions of

$$i - j$$

. In addition, the first term is positive for

$$y_0 > -y_c$$

and the second term is positive for

$$r_0 < R$$

, using

$$0 < R - r_0 \leq R - r_0 \cos(\varphi - \varphi') \qquad (64\text{a})$$

and

$$0 < (R - r_0)^2 = R^2 + r_0^2 - 2Rr_0$$
$$\leq R^2 + r_0^2 - 2Rr_0 \cos(\varphi - \varphi') \qquad (64\text{b})$$

Therefore,

$$\mathbf{G}_{ij}$$

is a positive, decreasing function of

$$i - j$$

for

$$y_0 > -y_c$$

and

$$r_0 < R$$
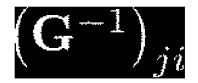
, and the determinant

$$\det \mathbf{G} = \sum_{\sigma \in S_{2n+1}} (\operatorname{sgn}\sigma)\, G_{-n,\sigma_{-n}} \cdots G_{n,\sigma_n} \qquad (65)$$

can be written as an alternating sum of decreasing terms.

Consequently,

$$\det \mathbf{G} \neq 0$$

and the inverse matrix

$$\left(\mathbf{G}^{-1}\right)_{ji}$$

exists.

[0047] For the second embodiment

$$\mathbf{G}_{ij} \underset{(23)}{\approx} \frac{\mu_0 Y \delta z}{2\pi \left[Y^2 + (\delta z)^2 (i-j)^2\right]}$$

$$- \frac{\mu_0 R^2 \delta z}{4\pi \left[R^2 + (\delta z)^2 (i-j)^2\right]^{3/2}} \left[(1 - 2\varepsilon_\varphi)\pi\right.$$

$$\left. + \left(\frac{3R^2}{R^2 + (\delta z)^2 (i-j)^2} - 1\right) \frac{l_x r_0 y_0}{R^3}\right] \quad (66)$$

under conditions (9) on

$$\left(x, y\right) = \left(x_0, y_0\right)$$

and using (63). Defining

$$W = (1 - 2\varepsilon_\varphi)\pi + \frac{2l_x r_0}{R^3} \min\{y_0, 0\} \quad (67)$$

$$\mathbf{G}_{ij}$$

is a positive, decreasing function of

$$i - j$$

for

$$0 \leq Y \ll R \quad (68)$$

and

$$n\delta z < \sqrt{\frac{RWy_0}{2}} \tag{69}$$

and the determinant

$$\det \mathbf{G}$$

(65) can be written as an alternating sum of decreasing terms. Consequently,

$$\det \mathbf{G} \neq 0$$

and the inverse matrix

$$\left(\mathbf{G}^{-1}\right)_{ji}$$

exists.

[0048] Using the inverse matrix

$$\left(\mathbf{G}^{-1}\right)_{ji}$$

, the equation

$$J_j \approx \sum_{i=-n}^{n} \left(\mathbf{G}^{-1}\right)_{ji} B_i \tag{70}$$

can be used to find

$$J_j$$

required to produce specified field values

$$B_i$$

.

[0049] Let

$$D$$

be such that

$$D \subset \{(x, y, z) : |z| < n \delta z\} \tag{71}$$

and let

$$\tilde{b}(z)$$

be a smooth function better approximating the ideal field

$$B^{\text{id}}$$

over

$$D \cap \Lambda$$

than (17), where

$$\Lambda$$

is the line

$$\Lambda = \{(x, y, z) : x = x_0, y = y_0\} \tag{72}$$

With

$$B_i = \tilde{b}(i \delta z) \tag{73}$$

values of

$$\tilde{b}(z)$$

,

$$J_j$$

can be calculated from (70) and a current density profile

$$J(z)$$

constructed by connect-the-dots. The smooth field

$$B(x, y, z)$$

(7) produced by

$$J(z)$$

better approximates

$$B^{id}$$

over

$$D$$

than (17).

4.3 ADJUSTABLE FIELD OF VIEW

[0050] The first and second embodiments can be designed with several fields of view

$$\eta_1 \tilde{L}_z < \eta_2 \tilde{L}_z < \cdots < \eta_N \tilde{L}_z \tag{74}$$

in mind. Let fields

$$G_z \tilde{z}_a$$

,

$$a = 1, \ldots, N$$

, approximate ideal fields (57) over

$$D$$

:

$$\tilde{z}_a|_D \approx \tilde{z}^{\text{id}}\left(z; \eta_a \tilde{L}_z\right)|_D \tag{75}$$

The notation

$$D$$

means restricted to

$$D$$

. Define fields

$$B_a$$

by

$$B_1 = G_z \tilde{z}_{a=1} \tag{76a}$$

and, for

$$a = 2, \ldots, N$$

,

$$B_a = G_z \left(\tilde{z}_a - \tilde{z}_{a-1}\right) \tag{76b}$$

Current density profiles

$$J_a(z)$$

producing fields approximating

$$B_a$$

can be found by the method of Sec. (4.2). With compo-
nents

$$a = 1, \ldots, N$$

carrying

$$J_a(z)$$

, the first

$$k \leq N$$

components generate a field

$$B^{(k)} = B_1 + \cdots + B_k = G_z \widetilde{z}_k \tag{77a}$$

with

$$B^{(k)}|_D \approx \widetilde{z}^{\mathrm{id}}\left(z; \eta_k \widetilde{L}_z\right)|_D \tag{77b}$$

5 ADVANTAGE OF LC COIL FOR MRI

[0051] The gradient of an LC coil with smaller fields outside the
field of view can be switched more rapidly without violat-
ing a bound on the field rate of change. Consequently,
larger regions of

$$k$$

-space can be covered within a given time.

[0052] It is to be understood that while the invention has been described in conjunction with the detailed description thereof, the foregoing description is intended to illustrate and not limit the scope of the invention, which is defined the scope of the appended claims. Other aspects, advantages, and modifications are within the scope of the following claims.

[0053] Having described the invention, and two preferred embodiments thereof, what I claim as new and secured by letters patent is: